Atmospheric Environment 123 (2015) 380–391

Contents lists available at ScienceDirect

Atmospheric Environment

journal homepage: www.elsevier.com/locate/atmosenv

Characteristics and source apportionment of $PM_{2.5}$ during a fall heavy haze episode in the Yangtze River Delta of China

Yang Hua [a, b], Zhen Cheng [a, c], Shuxiao Wang [a, b, *], Jingkun Jiang [a, b], Daren Chen [d], Siyi Cai [a, b], Xiao Fu [a, b], Qingyan Fu [e], Changhong Chen [f], Bingye Xu [g], Jianqiao Yu [h]

[a] State Key Joint Laboratory of Environment Simulation and Pollution Control, School of Environment, Tsinghua University, Beijing 100084, China
[b] State Environmental Protection Key Laboratory of Sources and Control of Air Pollution Complex, Beijing 100084, China
[c] School of Environmental Science and Engineering, Shanghai Jiao Tong University, Shanghai 200240, China
[d] Department of Mechanical and Nuclear Engineering, School of Engineering, Virginia Commonwealth University, VA 23284-3028, USA
[e] Shanghai Environmental Monitoring Center, Shanghai 200030, China
[f] Shanghai Academy of Environmental Sciences, Shanghai 200233, China
[g] Zhejiang Environmental Monitoring Center, Hangzhou 310015, China
[h] Jiangsu Environmental Monitoring Center, Nanjing 210036, China

HIGHLIGHTS

- The pollution exhibited temporal synchronization in the YRD and occurred in a regional scale.
- Organic matter, sulfate, nitrate, and ammonium were the dominant components of $PM_{2.5}$, and impact the visibility most.
- $PM_{2.5}$ mainly came from the secondary pollutants and the primary emissions of vehicles and biomass burning in this episode.
- A polluted air mass transported from the north Jiangsu Province and the stagnant meteorology further aggravated the haze.

ARTICLE INFO

Article history:
Received 16 December 2014
Received in revised form
19 March 2015
Accepted 22 March 2015
Available online 23 March 2015

Keywords:
Haze
$PM_{2.5}$
Source apportionment
Yangtze River Delta

ABSTRACT

Joint field observations were conducted from October to November in 2011 to observe haze pollution in the Yangtze River Delta (YRD), China. Samples of particulate matter with diameter less than 2.5 μm ($PM_{2.5}$) and less than 10 μm (PM_{10}), gaseous pollutants and meteorology data were collected in five cities – Shanghai, Suzhou, Nanjing, Ningbo and Hangzhou – in the YRD. The chemical composition of $PM_{2.5}$ was analyzed and the light extinction resulting from each chemical species was calculated using the IMPROVE algorithm. A typical heavy haze episode was selected and the chemical mass balance (CMB) model was applied to identify the sources of $PM_{2.5}$. The average $PM_{2.5}$ and PM_{10} mass concentrations during the haze episode were 100 ± 24 μg/m^3 and 164 ± 19 μg/m^3, respectively; visibility decreased to 1 km. Organic matter (OM), sulfate, nitrate, and ammonium were the dominant components of $PM_{2.5}$, accounting for 33%, 19%, 17% and 11% of $PM_{2.5}$ mass, respectively. Sulfate, OM and nitrate had the highest impact on light extinction, contributing 30%, 28% and 19%, respectively. The source apportionment indicate that $PM_{2.5}$ is primarily from secondary pollutants and primary emissions from vehicles and biomass burning. A polluted air mass from north Jiangsu Province and stagnant meteorology further aggravated the haze pollution. The five cities had similar characteristics and pollution sources.

1. Introduction

The Yangtze River Delta (YRD), including Shanghai city, Zhejiang Province and Jiangsu Province, is a rapidly developing region which accounts for 2.2% of the area of China and 21.5% of the Gross Domestic Product (GDP) in China. With rapid economic expansion, coal consumption has increased dramatically since 2000 and

* Corresponding author. State Key Joint Laboratory of Environment Simulation and Pollution Control, School of Environment, Tsinghua University, Beijing 100084, China.
E-mail address: shxwang@tsinghua.edu.cn (S. Wang).

http://dx.doi.org/10.1016/j.atmosenv.2015.03.046
1352-2310/

accounted for 16.6% of the national total coal consumption in 2010, resulting in severe regional air pollution (Fu et al., 2014).

The pollution characteristics and haze formation in the YRD have been studied by several researchers. Cheng et al. (2013) found visibility in the YRD declined from 13.2 km to 10.5 km between 1980 and 2000 while Gao et al. (2011) identified a 2.4 km decrease per decade between 1981 and 2005, indicating increasing particle pollution in the YRD. Haze pollution in the YRD occurs frequently and is often severe in both fall and winter seasons. Analysis of a haze episode in Nanjing – one of the YRD cities in this study – in the fall of 2009 suggested that high humidity, regional transport, local emissions and unfavorable diffusion were the major reasons for the haze. In this episode, the highest PM_{10} concentration reached 250–400 $\mu g/m^3$ in the YRD region (far in excess of 75 $\mu g/m^3$, the Interim Target-3 recommended by the World Health Organization, WHO) (Kang et al., 2013). Source apportionment in Shanghai – another YRD city in this study – in the fall of 2010 suggested the dominant contributor to haze events could be either local emissions or regional transport, depending on the meteorological conditions (Wang et al., 2014a). In the Shanghai winter season stagnant meteorological conditions with low wind speed, high humidity and weak radiation favored haze formation (Pan et al., 2010; Xiao et al., 2011). Heavy pollution was reported on January 19th, 2007: the daily average PM_{10} concentration reached 512 $\mu g/m^3$ in Shanghai and 280–470 $\mu g/m^3$ in other cities of the YRD (Liu et al., 2010). In general, the haze formation in the YRD is primarily attributed to the emissions of primary sub-micrometer particles and gaseous pollutants, unfavorable meteorology and pollution sources that vary by the season, such as biomass burning in fall. Moreover, in consideration of the fact that sulfate, nitrate, ammonium and organic aerosol are the dominant components of $PM_{2.5}$ in Shanghai, gas-to-particle conversion is also likely a significant contributor to haze formation in YRD (Yao et al., 2002; Wang et al., 2006; Ye et al., 2003; Yang et al., 2005; Feng et al., 2009). Particle hygroscopic growth from high humidity and biomass burning after harvests often leads to heavy pollution in winter (Zhang et al., 2012; Zhao et al., 2013). However, most studies focus on winter, while haze in fall is also severe and complicated. Further, studies of YRD air pollution usually review data from only one city, either Shanghai or Nanjing.

Very limited data have been reported for YRD regional pollution characteristics, especially in fall. It is, however, necessary to investigate the spatial distribution of pollutants and regional pollution transport in order to identify a short-list of potential pollution sources. Moreover, the detail formation mechanism of fall haze pollution is not well understood. In this article, we report the result obtained from field observations carried out in five cities of the YRD – Shanghai, Nanjing, Hangzhou, Suzhou and Ningbo – particularly on characteristics of a haze episode during the observation period (10/20/2011–11/30/2011). The similarity and differences of air pollution among different cities in this region are discussed, improving the understanding of regional particle pollution formation.

2. Methodology

2.1. Field observation

The field observations were conducted from October 20th to November 30th in 2011. The sampling sites were located in five cities –Shanghai, Suzhou, Nanjing, Ningbo and Hangzhou. Nanjing and Hangzhou are the capitals of Jiangsu and Zhejiang Provinces, respectively. Shanghai is a mega city surrounded by Jiangsu and Zhejiang Province. Shanghai and Hangzhou are located near the ocean. Ningbo and Nanjing are partially surrounded by mountains (see Fig. 1). Suzhou is located between Taihu Lake and Shanghai. Air masses are affected by the geography of this region: a polluted air mass from the north and northwest often results in regional air pollution while prevailing wind from the east carries clean air into the region. The observation sites were selected according to the frequency of pollution occurrences and field wind directions (Cheng et al., 2014).

All sites were located in residentially- and commercially-mixed areas without large industrial or dust sources nearby. The altitude range of all sites is about 5–30 m. Table S1 provides details of the sampling sites.

The observations included continuous monitoring of air pollutants and manual sampling of $PM_{2.5}$. Continuous monitoring included the mass concentration of $PM_{2.5}/PM_{10}$, meteorology (i.e., relative humidity (RH), temperature, and wind speed/direction), visibility, chemical composition of $PM_{2.5}$ and concentrations of SO_2, NO_x, and O_3 (Table S1). All the data were captured as hourly values. $PM_{2.5}/PM_{10}$ mass concentration was determined by the TEOM method.

$PM_{2.5}$ samples were manually collected on 47 mm quartz and Teflon filters (Whatman, UK) by Partisol 2300 (Thermo, USA) every 22 h (beginning at 14:00 pm and ending at 12:00 pm the following day; local standard time (LST)) at all the sites. Teflon filters were loaded in Channel 1 (rate: 16.7lpm) for mass concentration measurement and elemental analysis. Quartz filters were loaded in Channel 2 (rate: 10lpm) for OC/EC measurement and inorganic water-soluble ions analysis. Filter masses were determined by using the standard gravimetric mass method in the laboratory. Elements including Al, As, Br, Ca, Cr, Cu, Fe, Mn, Ni, Pb, Rb, Se, Si, Sr, Ti and Zn were analyzed by x-ray fluorescence (XRF) (Yang et al., 2011; Harper et al., 2005). OC and EC concentrations were determined using a thermal/optical aerosol carbon analyzer (Model 2001A, DRI, USA). The IMPROVE_A thermal-optical reflectance protocol was applied for the analysis (Chow et al., 2011). Organic matter (OM) was estimated by multiplying OC by a factor of 1.55 (Huang et al., 2012). Soil was calculated as the sum of Al, Si, Ti, Ca and Fe (Lowenthal and Kumar, 2003). Particles on filters were extracted in an ultrasonic bath (Wang et al., 2006). Soluble ions – SO_4^{2-}, NO_3^-, Cl^-, F^-, NH_4^+, Na^+, K^+, Ca^{2+} and Mg^{2+} – were analyzed by the Dionex Ion Chromatograph System (ICS-3000). Non-soil K^+ which is related to biomass burning was calculated by using the water-soluble K^+ minus 0.6*[Fe] (Hand, 2011; Ye et al., 2003). The detailed quality assurance and quality control (QA/QC) of chemical analyses were reported in our previous paper (Cheng et al., 2014).

2.2. Satellite and meteorological data

The locations of open burning sites were obtained from the Fire Information for Resource Management System (FIRMS) (http://firms.modaps.eosdis.nasa.gov/firemap/), which were further verified by comparing that information with the cloud cover information obtained from the Moderate Resolution Imaging Spectroradiometer (MODIS) atmosphere observation (http://earthdata.nasa.gov/labs/worldview/).

Weather patterns were from the Hong Kong Observatory (http://www.hko.gov.hk/cgi-bin/hko/dwm_c.pl). The Hybrid Single Particle Lagrangian Integrated Trajectory (HYSPLIT) model was run in a 24-h back-trajectory mode at 50, 100 and 500 m starting from each site to analyze the potential source areas. Planetary boundary layer (PBL) height was obtained from the Global Data Assimilation System (GDAS) model (http://www.ready.noaa.gov/READYamet.php).

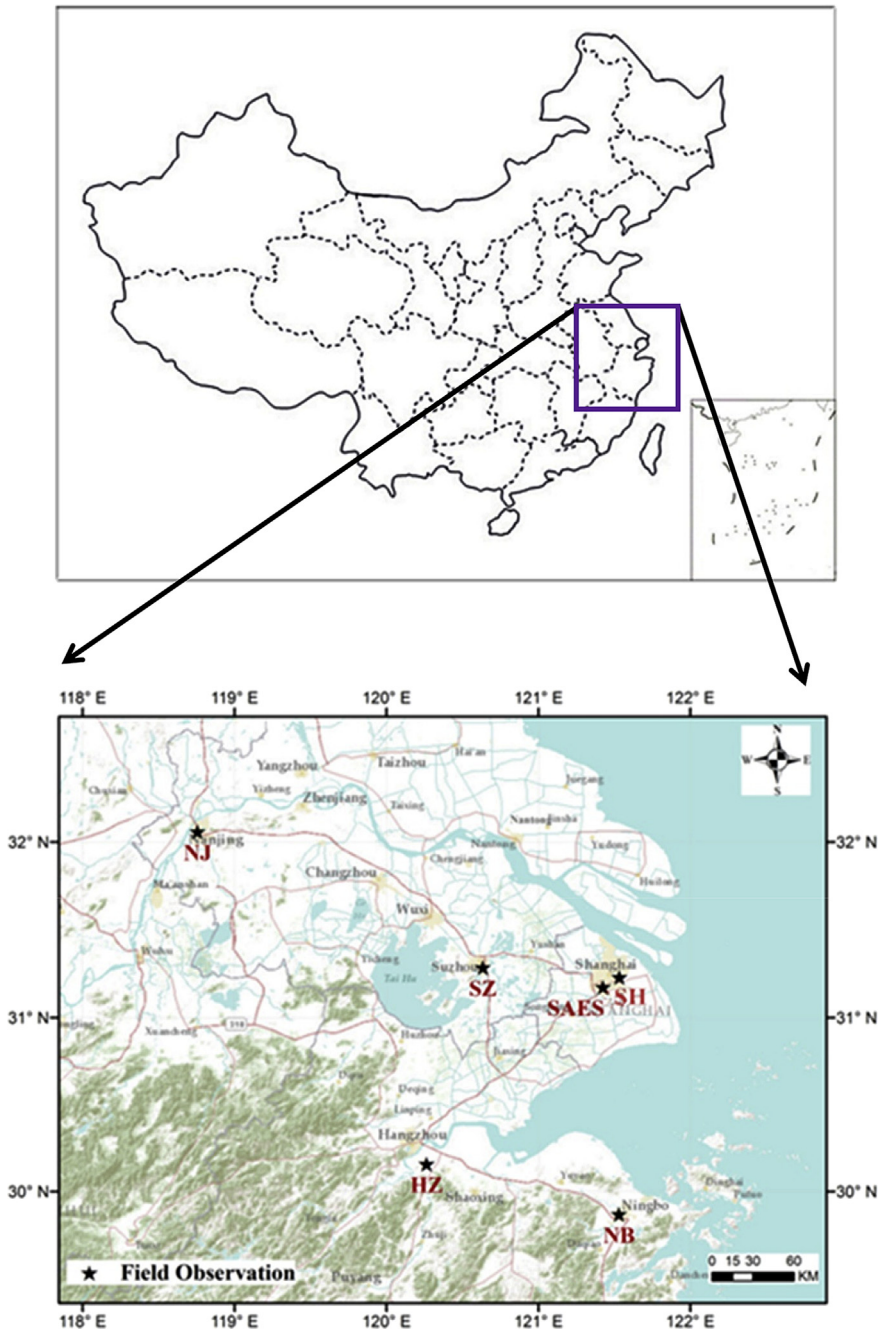

Fig. 1. Locations of field observation sites. *NJ, SZ, SH, SAES, HZ and NB represent Nanjing, Suzhou, Shanghai, Shanghai Academy of Environmental Sciences, Hangzhou and Ningbo.

2.3. Chemical mass balance (CMB) model

CMB8.2 from the US Environmental Protection Agency (EPA) was used to identify the sources of $PM_{2.5}$ in each city. The source profiles used in this study were summarized from the literature. Nine source categories were identified, including industrial coal combustion, residential gas combustion, residential biomass burning, iron and steel manufacturing, vehicles, dust, open biomass burning, secondary sulfate and secondary nitrate. Since CMB doesn't distinguish secondary sources, "pure" sulfate (contains only 72.7% sulfate ion in $(NH4)_2SO_4$) and "pure" nitrate (contains only 77.5% nitrate ion in NH_4NO_3) are assumed as secondary sources in the source profile. As a result, the method identifies the contribution of gas-to-particle formation (Wu et al., 2014). In total, 22 species, including various chemical elements, carbonaceous matters and water soluble ions, were used in the source apportionment. The model analysis was conducted for each of the five cities.

2.4. Calculation of light extinction coefficient

The extinction coefficient was apportioned by the IMPROVE extinction coefficient equation (Eq. (1)) of the revised version (Pitchford et al., 2007). $PM_{2.5}$ data were obtained from the manual samples and PM_{10} data were from the Ministry of Environmental Protection of China (http://datacenter.mep.gov.cn/). It is noticed CM

contribution only 1%–5% to the total extinction coefficient for the cities in this study. In this case, the random error resulting from the difference of PM_{10} and $PM_{2.5}$ data sources affects little the results of extinction coefficient (Figure S1).

$$\begin{aligned} Bext = {} & 2.2 \times f\_S(RH) \times [small\ (NH_4)_2SO_4] + 4.8 \times f\_L(RH) \\ & \times [large\ (NH_4)_2SO_4] + 2.4 \times f\_S(RH) \times [small\ NH_4NO_3] \\ & + 5.1 \times f\_L(RH) \times [large\ NH_4NO_3] + 2.8 \times [small\ OM] \\ & + 6.1 \times [large\ OM] + 10 \times [EC] + 1 \times [soil] + 1.77 \\ & \times [sea\ salt] + 0.6 \times [CM] + Rayleigh + 0.33 \times [NO_2] \end{aligned} \quad (1)$$

The IMPROVE formula for light extinction (b_{ext}) calculates extinction in units of inverse mega-meters (Mm^{-1}). The total light extinction results from the light scattering and absorption of particles and light scattering by gases. Light scattering by particles arises from $(NH_4)_2SO_4$, NH_4NO_3, organic matter (OM), soil dust, and coarse matter (CM). The formula also takes into the consideration the light extinction due to chemical composition in small and large particle size ranges. For composition X (X represents $(NH_4)_2SO_4$, NH_4NO_3 and OM), the small and large part concentration can be calculated as follows:

$$[Large\ X] = [Total\ X]^2 \Big/ 20, \text{ for } [Total\ X] < 20\mu g/m^3$$

$$[Large\ X] = [Total\ X], \text{ for } [Total\ X] \geq 20\mu g/m^3$$

$$[Small\ X] = [Total\ X] - [Large\ X]$$

3. Result and discussion

3.1. Characteristics of air pollution

3.1.1. Visibility and concentration of particulate matter (PM)

Visibility and RH are used to define haze days. A haze day has daily average RH <80% and daily average visibility <10 km (China Meteorological Administration, 2011). Non-haze days are those with RH <80% and visibility ≥10 km. Days with RH ≥ 80% are not considered because it's difficult to distinguish the cause of low visibility. Data were missing in the Nanjing site for non-haze days. The heavy haze pollution in the YRD occurred from November 10th to 15th, 2011, thus was selected as the pollution episode for this study.

Figure S2 and Fig. 2 show the particle concentration and visibility during the haze episode. More statistical data of pollutants are provided in the Table S2. The average concentrations of $PM_{2.5}$ and PM_{10} during non-haze days from October 20th to November 30th, 2011 were 24–44 μg/m^3 and 40–86 μg/m^3, respectively. During the haze episode, the average concentrations of $PM_{2.5}$ and PM_{10} were 63–128 μg/m^3 and 140–189 μg/m^3, respectively. The $PM_{2.5}$ concentration reached a peak of 450 μg/m^3 in Shanghai, compared with 140–190 μg/m^3 in the other cities. The concentration of particles kept increasing for several days in each of the five cities and peaked during the time from the midnight of November 13th to the noon of November 14th. The particle concentration significantly increased the night of November 13th, especially in Shanghai, where the average change in $PM_{2.5}$ concentration was 45 μg/m^3/h in the 6 h before the peak, much higher than in the other four cities. For the other cities, the growth rates of hourly $PM_{2.5}$ concentration on November 13th were 12, 28, 27 and 13 μg/m^3/h in Nanjing, Ningbo, Suzhou and Hangzhou, respectively.

Visibility dramatically decreased during the episode. The average YRD visibility in non-haze days and the haze episode were 14–26 km and 3–7 km, respectively. The visibility was lower than 2.5 km at the peak of $PM_{2.5}$ concentration. In Shanghai, the visibility at the peak of the $PM_{2.5}$ concentration was less than 1 km and the ratio of $PM_{2.5}/PM_{10}$ was greater than 90%.

Figures S3–S5 show the relationship of $PM_{2.5}$ concentration, PM_{10} concentration, RH and visibility, respectively. The curves fit are also included in the figures. Visibility decreased with the increase of $PM_{2.5}$ and PM_{10} concentration in all five cities. The correlation of PM_{10} and visibility is lower than that of $PM_{2.5}$. What's more, with particle concentration increases, the impact of RH on the visibility gets relatively lower and visibility decreases at a lower rate. Compared with the other cities, the power index of the curve fit was much larger for Shanghai. The ratio of $PM_{2.5}/PM_{10}$ and $PM_{2.5}$ concentration were much higher in Shanghai, indicating secondary particle composition accounting for a large proportion in $PM_{2.5}$, including sulfate and nitrate. These compositions have a very significant impact on the visibility, according to the IMPROVE algorithm.

The pollution episode exhibited a temporal synchronization among all sampling sites, inferring that common causes for the haze existed in the region. However, different pollution characteristics were observed in five cities including different ratios of $PM_{2.5}/PM_{10}$, mass concentration of particles and visibility range. For example, Shanghai experienced the highest $PM_{2.5}$ concentration (450 μg/m^3), the highest ratio of $PM_{2.5}/PM_{10}$ (90%), and the lowest visibility (1 km) compared with the other cities.

3.1.2. Concentration of gaseous pollutants

During the haze episode, the SO_2, NO_2 and O_3 concentrations were 30–80 μg/m^3, 30–150 μg/m^3 and 30–50 μg/m^3, respectively. Concentrations of SO_2 and NO_2 in the haze episode were 1.64 and 1.33 times the concentrations in non-haze days (see Figure S6).

Fig. 3 shows the concentration of gaseous pollutants during the haze episode in all the cities. The peak for gaseous pollutants occurred earlier than that for particles, indicating the gas-to-particle conversion might be dominant in Shanghai's haze formation.

The temporal variation of SO_2 differed among the five cities while NO_2 was similar in all cities. The SO_2 concentration in Shanghai, Suzhou and Nanjing reached its peaks at noon November 13th while the peaks were different in the other cities. The temporal variations of NO_2 concentration in the five cities were similar to each other. This indicates the NO_2 emission sources were similar at the regional scale. In 2010, power plants, on-road transportation and industrial combustion were the largest emission sources of NO_x in the YRD. Power plants and industrial combustion also made the largest contribution to the emissions of SO_2 because of coal combustion (Huang et al., 2013). It can be inferred that the observed difference between SO_2 and NO_2 resulted from on-road transportation NO_2 emissions.

The diurnal variation of both SO_2 and NO_2 concentrations in the five cities were similar to each other. The highest SO_2 concentration occurred in the daytime. Other research has shown that the YRD SO_2 concentration peaked at midnight from 2005 to 2009, but peaked in the daytime from 2009 to 2010 (Qi et al., 2012). The highest NO_2 concentration occurred at midnight and the lowest at noon in the five cities during the episode. Therefore, it is reasonable to attribute the NO to anthropogenic sources in the day that are later transformed into NO_2, which is accumulated near the ground under unfavorable diffusion conditions during night-time.

The temporal variation of O_3 concentrations differed among the five cities. The photochemical process became stronger during the episode in Nanjing, Ningbo and Hangzhou, but weaker in Suzhou.

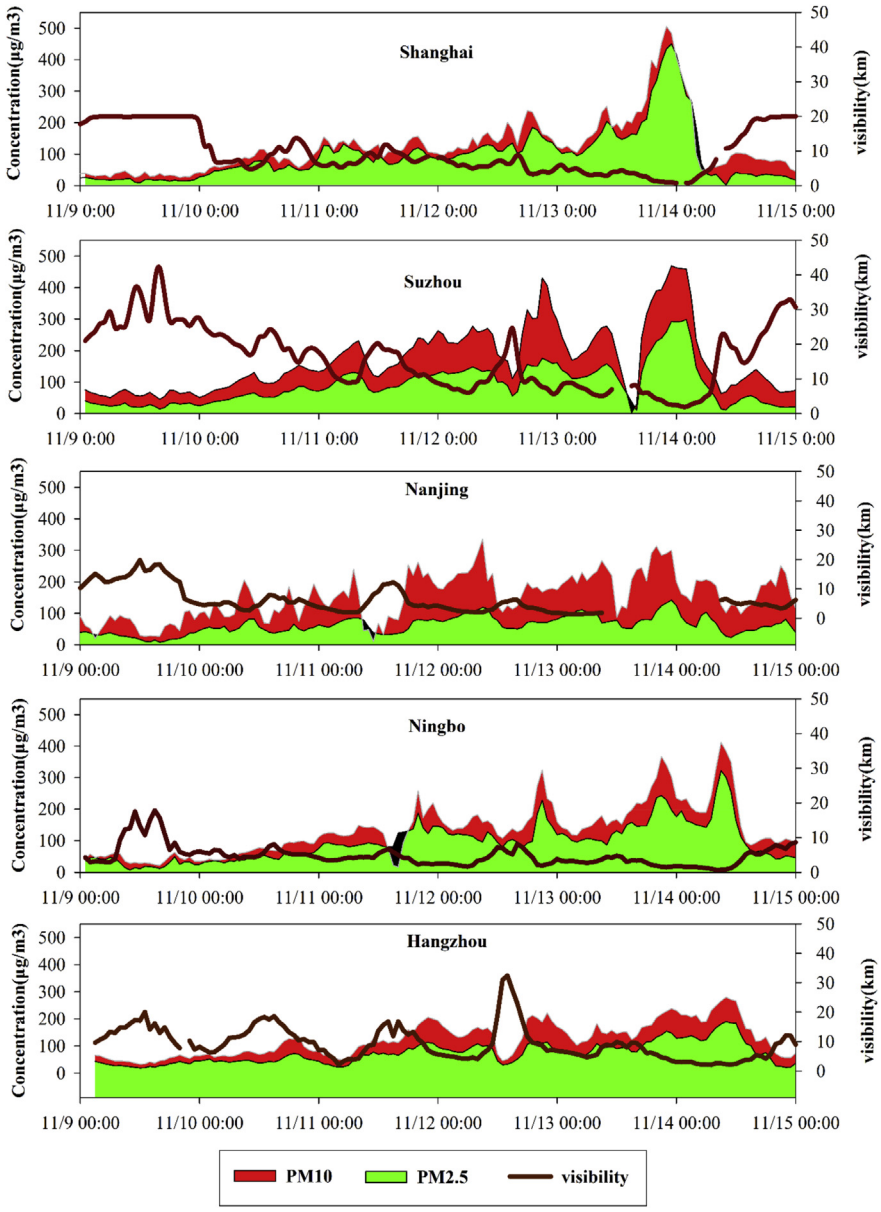

Fig. 2. Particle concentration and visibility during the haze episode.

The O_3 concentration had a less obvious change during the pollution episode in Shanghai. The above observation indicates the pollution processes might be different among the cities.

3.1.3. *Chemical compositions of $PM_{2.5}$*

During the haze episode, the dominant components of $PM_{2.5}$ were OM, SO_4^{2-}, NO_3^- and NH_4^+, accounting for 33%, 19%, 17% and 11% of the total, respectively. Similar results were reported in the Pearl River Delta (PRD) of China (Wang et al., 2014b). On non-haze days, average concentrations of EC, OM, NH_4^+, K^+, SO_4^{2-} and NO_3^- were 3.82 ± 1.48, 16.87 ± 6.86, 5.17 ± 1.86, 0.45 ± 0.30, 8.31 ± 1.76 and 6.02 ± 1.98 μg/m^3, respectively. During the episode, the average concentrations of EC, OM, NH_4^+, K^+, SO_4^{2-} and NO_3^- in the five cities were 7.60 ± 1.36, 40.78 ± 9.04, 14.00 ± 2.15, 1.49 ± 0.36, 24.05 ± 5.05 and 23.14 ± 4.59 μg/m^3, respectively. More statistical data of chemical components of $PM_{2.5}$ are provided in the Table S3. As shown in Fig. 4, the increase of OM, EC and SO_4^{2-} in the five cities was comparable (approximately 1–4 times in OM, 1–3 times in EC and 2–4 times in SO_4^{2-}). Potassium (K^+), usually regarded as a tracer for biomass burning, increased 11 times in Shanghai and 2–4 times in the other cities during the haze episode, indicating biomass burning was a significant source during this episode. At the same time, nitrate increased 8 times in Shanghai and 2–4 times in other cities, and ammonium increased 5 times in Shanghai and 2–3 times in the other cities. Considering the relatively stable emissions from the primary sources, the extremely high increase of NO_3^- in Shanghai was probably from secondary particle formation.

3.2. *Formation of a haze episode*

3.2.1. *Effect of meteorological condition*

Prior to the haze pollution event, the YRD region was located at the front of a high pressure system. Prior to November 14th, the atmosphere was in steady state with increasing atmospheric pressure, weak wind and high temperature. The wind was also weak on November 12th and 13th. The average wind speed was 0.67,

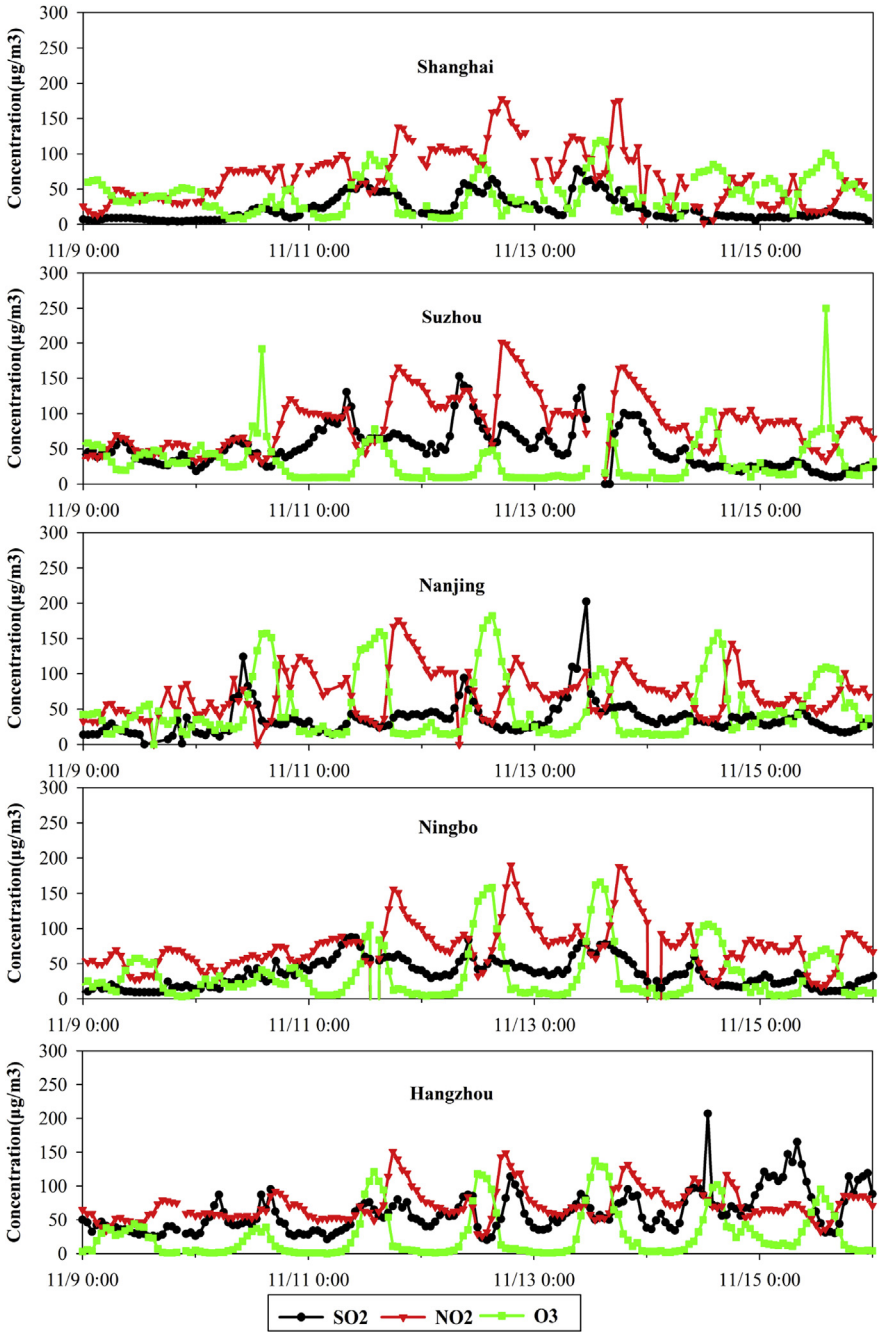

Fig. 3. Concentrations of gaseous pollutants during the haze episode.

0.65, 1.34, 0.84 and 1.04 m/s in Shanghai, Suzhou, Nanjing, Ningbo and Hangzhou, respectively. On November 14th, the average wind speed increased to 1.26, 1.06, 1.71, 1.26 and 1.01 m/s in Shanghai, Suzhou, Nanjing, Ningbo and Hangzhou, respectively (see Fig. 5). The daily average wind speed was 0–2 m/s for 42.4% of haze days from 1990 to 2011 in Shanghai (Qing and Jun, 2010). Compared to the wind speed during non-haze days, the wind speed was much lower during the haze episode. Similar to the wind speed, the planetary boundary layer (PBL) in Shanghai, Suzhou, Ningbo and Hangzhou was low on November 12th and 13th and higher on November 14th (see Fig. 6). The low wind speed and low PBL led to pollutant accumulation near the surface. During the haze episode, the dominant wind directions were different in the five cities. The wind directions in Shanghai and Ningbo were primarily from the northwest (NW) and southeast (SE), respectively. It indicates that the pollution in Shanghai was probably from Jiangsu and Anhui provinces.

The temperature in all the cities increased on November 12th and 13th, and then decreased on November 14th. For example, the highest temperatures in Hangzhou were 20.38 °C and 18.23 °C on November 13th and 14th, respectively. Pollutants accumulated near the surface under stagnant meteorological conditions and high temperature promoted gas-to-particle transformation in the YRD region. Moreover, the average RH was 63%–69% in the five cities during the episode and the highest RH was about 80%. The relative humidity in Shanghai also experienced a sharp increase from the afternoon of November 13th to the early morning of November 14th, facilitating a heterogeneous reaction in the atmosphere (it also

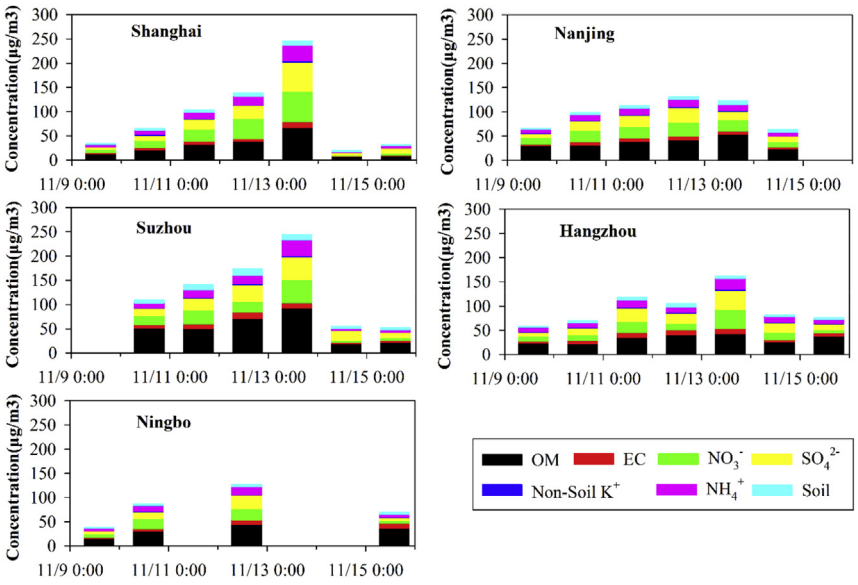

Fig. 4. Chemical composition of $PM_{2.5}$ in the YRD during the haze episode. *Chemical composition of $PM_{2.5}$ in SAES was obtained from continuous monitoring and K^+ concentration is the original data instead of non-soil K^+ due to lack of Fe concentration.

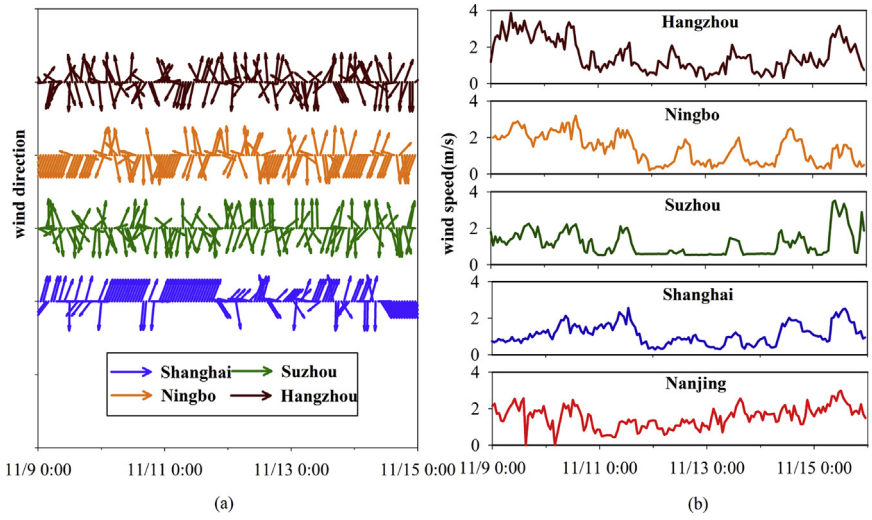

Fig. 5. Wind direction and speed during the haze episode. *(a) is the wind direction of the four cities. Directions of arrows represent wind directions. The arrow direction in the legend represent 0° (north direction). Meanwhile, in the clockwise direction, 90, 180, 270° represent east, south and west direction, respectively. Data of wind direction in Nanjing is lost. (b) shows the wind speed.

explains the observation of extremely high concentrations of particles and ratio of $PM_{2.5}/PM_{10}$ during the episode). The significant increase of RH in Shanghai preceding the pollution peak was probably the external cause of the rapid growth of $PM_{2.5}$ pollution in Shanghai. On November 14th a strong cold air mass moving towards the south resulted in strong wind and rapid pollution diffusion.

3.2.2. *Effect of biomass burning*

The backward trajectory analysis showed that the air mass from northern Jiangsu Province, where open biomass burning was observed, moved to the observation region on November 12th (Fig. 7). A previous study found that in 2010 biomass burning accounted for about 10% and 20% of primary emission of $PM_{2.5}$ and PM_{10} in the YRD region, respectively (Fu et al., 2013). The above values are for the whole year and expected to be much higher during short time periods. Usually biomass burning is concentrated from late May to early June and from late October to early November (when rice and wheat are harvested). The particulate pollutant concentration started to increase on November 12th, indicating open biomass burning was an important pollution source. The $PM_{2.5}$ concentration increased remarkably in Nanjing, Suzhou and Hangzhou on November 12th. The effect of regional transport continued in the YRD region and Anhui province on November 13th. The concentration of K^+ on November 13th was 3 times that on the 12th. The K^+ concentration increased the most in Shanghai while no obvious open fire was observed in the area, indicating the largest impact was air mass transport into Shanghai. On November 14th, the direction of air mass transport changed to the northeast (NE), carrying clean air from the ocean to the YRD region. The particles concentration experienced a rapid decline. The increase of K^+

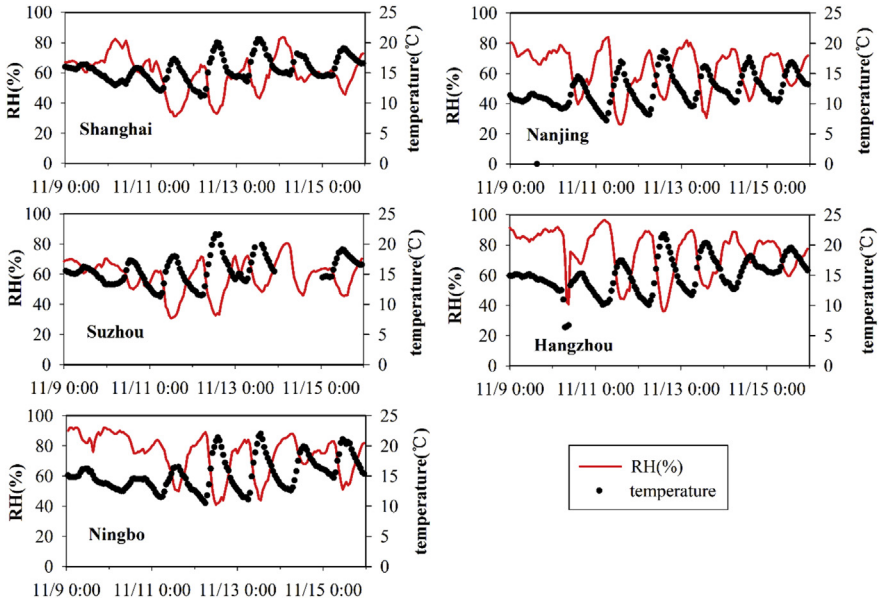

Fig. 6. Relative humidity and temperature during the haze episode.

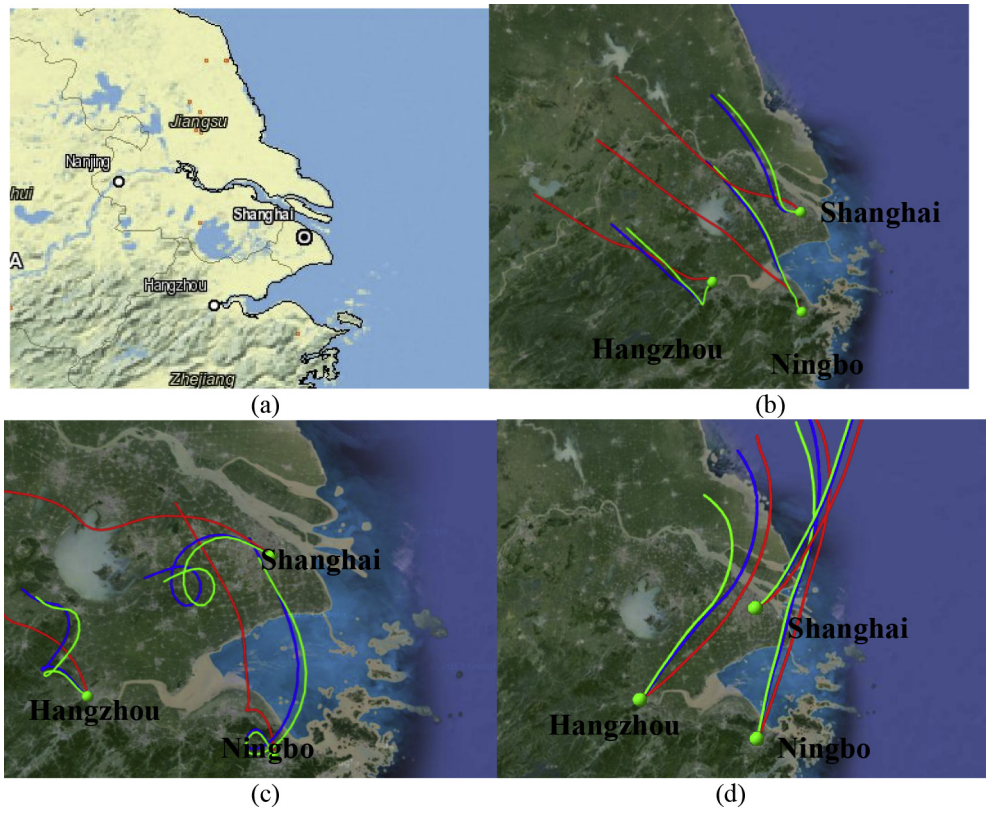

Fig. 7. Fire points and backward trajectory during the haze episode. (a) is the fire point map observed by satellite. (b), (c), (d) are the backward trajectories of Shanghai, Hangzhou and Ningbo on 12, 13, 14 November at 0000 UTC, which is 0800 LST. The backward trajectories of Suzhou and Nanjing were similar to those in Fig. 7. The red, blue and green lines represent the trajectories of 50 m, 100 m and 500 m AGL, respectively. (For interpretation of the references to colour in this figure legend, the reader is referred to the web version of this article.)

indicates that pollutants emitted from open biomass burning were transported across the region and significantly contributed to the heavy pollution episode. Similar transport in the YRD region was also reported in Nanjing in October, 2009 (Kang et al., 2013).

3.2.3. Source apportionment of $PM_{2.5}$

The source apportionment results obtained from the CMB model are given in Fig. 8. Hangzhou showed some sources' contributions are negative values, which may result from source profile collinearity or source contributions close to zero. The possibility is

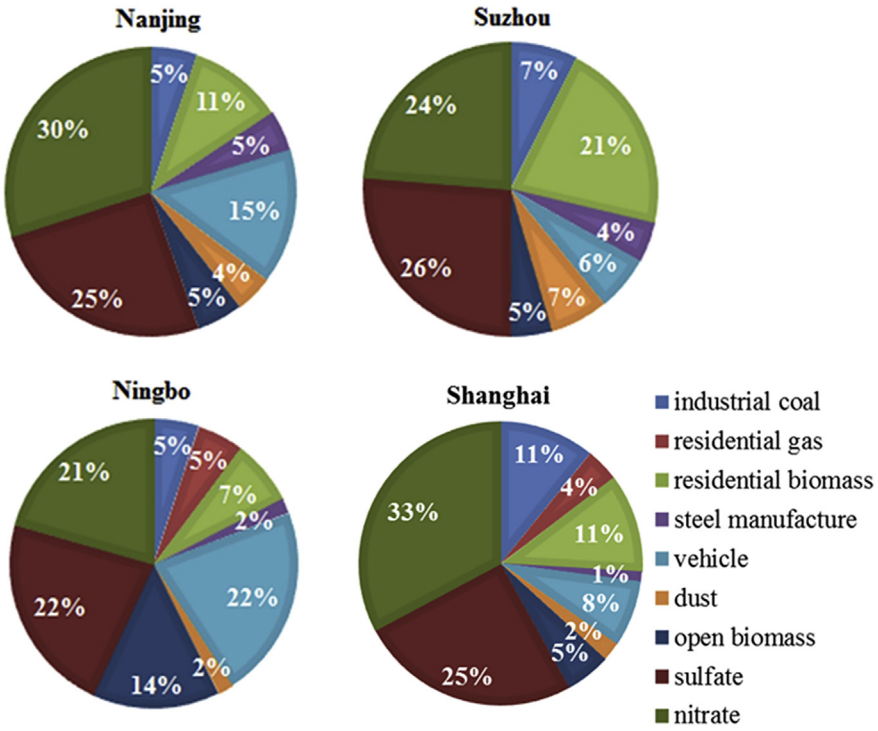

Fig. 8. Contribution of various sources to $PM_{2.5}$ from November 10th to 15th, 2011. *The source name is abbreviated because of space limitation. Industrial coal refers to industry coal combustion; residential gas refers to residential natural gas combustion; residential biomass refers to residential biomass burning; steel manufacture refers to iron and steel manufacture; open biomass refers to open biomass burning; sulfate refers to secondary sulfate; nitrate refers to secondary nitrate.

very low that more than one source's contributions are close to zero. However, eligible space collinearity displayed in the model shows no potential source collinearity. Another possible explanation for the negative values might be a standard error larger than the source contribution estimates.

Gas-to-particle conversion is the largest contributor to the $PM_{2.5}$ concentration. In general, contributions of primary sources are less than results obtained from "traditional" source profiles, which do not consider secondary sulfate and nitrate. Ranking the contributions of primary sources provides different results among the five cities. Vehicles were the most significant primary source for Ningbo, accounting for 22% of the contribution. Biomass burning (including that in the northern part of Jiangsu Province and from residential activities) was the largest primary pollution source for Nanjing, Shanghai and Suzhou, accounting for 16%, 16% and 26%, respectively. These results are consistent with our analysis from Section 3.1.

The sources of different chemical species varied significantly (Table S4). Residential biomass burning and vehicles contributed the largest amount to OM. Vehicles and dust were the major pollution sources for EC. The secondary inorganic ions mainly came from the gas-to-particle conversion process, especially for NO_3^- (over 97% from the chemical reaction). The results vary from those reported during a fall haze in 2010 in Shanghai (Wang et al., 2014a). The contribution of biomass burning is much larger, which is probably transported from the surrounding areas.

The gas-to-particle conversion contributed 58% of $PM_{2.5}$ in Shanghai, which further explains the low concentration of gaseous pollutants and the high $PM_{2.5}$ concentration. The significant increase in the concentration of K^+ further indicates that open biomass burning was the large primary source during this episode.

To explain the large contribution of gas-to-particle conversion, the nitrogen oxidation ratio (NOR) and sulfur oxidation ratio (SOR) are calculated. NOR (the ratio of $[nNO_3^-]$ to $[nNO_3^- + nNO_2]$, where n refers to molar concentration) and SOR (the ratio of $[NSO_4^{2-}]$ to $[nSO_4^{2-} + nSO_2]$) have been used to estimate the degree of oxidation of nitrogen and sulfur (Tan et al., 2009). The NOR and SOR values during the episode and non-haze days were calculated using the data obtained from Shanghai (Figure S7). The average NOR value during the episode and non-haze days was 0.18 and 0.084, respectively, indicating a much more active gaseous reaction during the haze pollution. Studies conducted in Tianjin and Guangzhou reported NOR values of 0.40 and 0.15 in winter, respectively (Zhao et al., 2013; Tan et al., 2009). In Beijing and Shanghai, nitrate is probably formed via heterogeneous hydrolysis of N_2O_5 under high humidity conditions (Pathak et al., 2009; Wei et al., 2015). Heterogeneous reactions might thus play an important role during this episode. The average of the SOR value, however, did not change significantly during the episode. Various mechanisms, primarily involving gas-phase oxidation and heterogeneous reaction, had been reported for the conversion of SO_2 to sulfate. Previous studies show that weak photochemical process and high NO_2 concentrations cannot produce sufficient conversion oxidants for sulfate production (Hua et al., 2008). This might be the reason for the weak sulfate conversion from SO_2 and little change of SOR during the episode.

3.2.4. Light extinction due to particles

The extinction coefficient of particles was calculated with the IMPROVE algorithm to identify the chemical composition effects on visibility. Sulfate, OM and nitrate mainly affect light extinction during both haze and non-haze days. During non-haze days, sulfate, OM and nitrate contributed to 28%–39%, 15%–25%, and 18%–32% of the total light extinction, respectively (the amount varied among the five cities). On average, sulfate, OM and nitrate contributed 30%, 28% and 19% during the haze episode, respectively. The extinction coefficient increased during the haze episode

in all of the five cities. Similar to particle concentration, the extinction coefficient increased dramatically in Shanghai and Suzhou while increasing little in the other cities. Compared to other reported cities (Table 1) (Brewer and Moore, 2009), the total extinction coefficients in the YRD region were much larger. In general, the contribution by dominant chemical components to light extinction during the episode was increased for nitrate and OM (Table S5). The above observation demonstrates the significant impact of secondary particles on visibility impairment.

Source apportionment of $PM_{2.5}$ chemical components was calculated along with the contribution of single chemical components. These results can be used to calculate contributions of sources to the particle extinction coefficient (Fig. 9).

$$R_{i,n} = S_{i,n} \times E_i \times 100\%$$
$$R_n = \sum_{i=1}^{4} R_{i,n} \quad (2)$$

i = 1, 2, 3, 4 (chemical components: sulfate, nitrate, OM, EC)
n = 1, 2, 3, 4, 5, 6, 7, 8, 9 (sources identified in the source apportionment)
$R_{i,n}$: contribution of a single chemical component from a single source to particle extinction coefficient
$S_{i,n}$: contribution of a single source to single chemical component concentration
E_i: contribution of a single chemical component to particle extinction coefficient
R_n: contribution of a single source to particle extinction coefficient

No source apportionment is identified for coarse particles, soil, sea salt and NO_2. These sources explain much of the 12%–19% of the extinction coefficient that is undefined. Generally, the source apportionments for $PM_{2.5}$ concentration and particle extinction are similar. Secondary particle formation has the largest impact on visibility in the whole region. To increase visibility, control strategies to reduce secondary particle formation will be necessary.

4. Conclusion

Regional-scale field observations for haze pollution were carried out to provide scientific support for regional pollution control efforts. Similar characteristics of haze pollution in the five cities (i.e., Shanghai, Nanjing, Hangzhou, Suzhou and Ningbo) were observed. During the haze episode, the particulate concentration significantly increased and exhibited temporal synchronization among the five cities. Gaseous pollutants also increased dramatically during the episode. The diurnal variation of gaseous pollutant concentrations was similar among the cities. The dominant components of $PM_{2.5}$ were OM, SO_4^{2-}, NO_3^- and NH_4^+. The secondary inorganic ions increased significantly during the haze episode and had the largest impact on visibility impairment. At the same time, a distinction of haze characteristics existed among the five cities. Shanghai experienced the highest $PM_{2.5}$ concentration (450 μg/m^3), the highest ratio of $PM_{2.5}/PM_{10}$ (90%), the lowest visibility (1 km) and the highest increase in NO_3^-, NH_4^+ and K^+ concentrations as compared with the other cities. The temporal variation of SO_2 and O_3 concentrations differed in various cities while the NO_2 concentration was similar in the region.

Transport of pollution from biomass burning in the north of Jiangsu province was observed in the cities on November 12th and had a significant impact on air quality in Shanghai. The stagnant meteorological factors (i.e., low wind speed, high temperature and thin PBL) were external reason for the pollution in the region following the arrival of the polluted air mass. The high emissions of pollutants from vehicles and local residential activities were the internal causes of pollution. Vehicle emissions and biomass burning (including pollutants carried by the regional transport and emitted by local residential activities) were the most important primary sources of $PM_{2.5}$. The gas-to-particle conversion process played an important role in the haze pollution formation (43%–58%). However, the details of pollution formation mechanisms differed in the five cities. The gas-to-particle conversion affected Shanghai's air pollution the most, primarily attributed to the dramatic increase of RH right before the peak $PM_{2.5}$ concentration. The transported pollutants also impacted Shanghai's air quality more than it did other cities.

The characteristics of pollution and source apportionment were similar in the YRD region. Although the meteorological factors led

Table 1
Comparison of extinction coefficient in different cities.

City name	Time period	Extinction coefficient (Mm^{-1})
Shanghai	Non-haze days	183.3
	Haze days	713.6
Nanjing	Non-haze days	669.4
	Haze days	789.1
Suzhou	Non-haze days	361.1
	Haze days	924.3
Ningbo	Non-haze days	664.9
	Haze days	766.6
Hangzhou	Non-haze days	425.2
	Haze days	883.7
Grand Canyon	20% haziest days (2000–2004)	34.6
	20% clearest days (2000–2004)	12.5
Agua Tibia	20% haziest days (2000–2004)	107.4
	20% clearest days (2000–2004)	26.7
Sawtooth	20% haziest days (2000–2004)	42.8
	20% clearest days (2000–2004)	15.0
Great Smoky Mtns.	20% haziest days (2000–2004)	216.3
	20% clearest days (2000–2004)	40.2
Cape Romain	20% haziest days (2000–2004)	147.3
	20% clearest days (2000–2004)	42.4
Everglades	20% haziest days (2000–2004)	116.4
	20% clearest days (2000–2004)	32.3

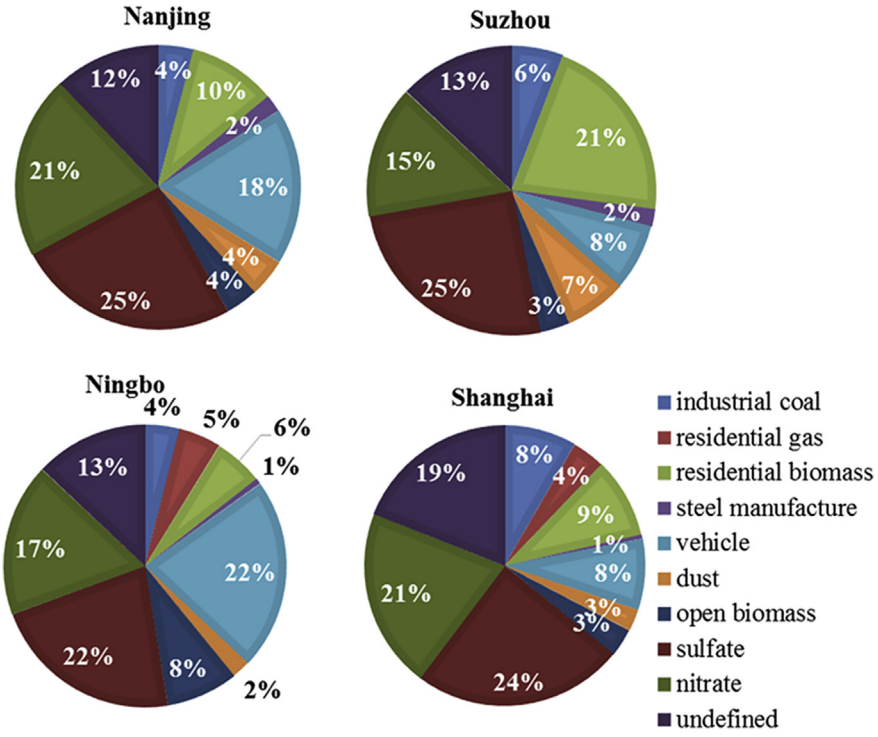

Fig. 9. Contribution of various sources to particle extinction coefficient from November 10th to 15th, 2011.

to the haze pollution, the high emissions of pollutants from the local area were the most important factor. In the future, studies on the formation of the secondary particles should be conducted as they significantly impact visibility and atmospheric pollution in the YRD region. The pollution transport trajectory in the region also needs more study in order to better understand this mechanism.

Acknowledgment

This work was sponsored by National Natural Science Foundation of China (21221004), Strategic Priority Research Program of the Chinese Academy of Sciences (XBD05020300), MEP's Special Funds for Research on Public Welfares (201409002) and the Collaborative Innovation Center for Regional Environmental Quality. The authors would like to thank Dr. Jeremy Schriefels from US EPA and Mr. Charles Freed for their help on language editing.

Appendix A. Supplementary data

Supplementary data related to this article can be found at http://dx.doi.org/10.1016/j.atmosenv.2015.03.046.

References

Brewer, P., Moore, T., 2009. Source contributions to visibility impairment in the Southeastern and Western United States. J. Air & Waste Manag. Assoc. 59 (9), 1070–1081.
Cheng, Z., Wang, S., Jiang, J., Fu, Q., Chen, C., Xu, B., Yu, J., Fu, X., Hao, J., 2013. Long-term trend of haze pollution and impact of particulate matter in the Yangtze River Delta, China. Environ. Pollut. 182, 101–110.
Cheng, Z., Wang, S., Fu, X., Watson, J., Jiang, J., Fu, Q., Chen, C., Xu, B., Yu, J., Chow, J., 2014. Impact of biomass burning on haze pollution in the Yangtze River delta, China: a case study in summer 2011. Atmos. Chem. Phys. 14 (9), 4573–4585.
China Meteorological Administration, 2011. Observation and Forecasting Levels of Haze; QX/T, pp. 113–2010.
Chow, J., Watson, J., Robles, J., Wang, X., Chen, L.W.A., Trimble, D., Kohl, S., Tropp, R., Fung, K., 2011. Quality assurance and quality control for thermal/optical analysis of aerosol samples for organic and elemental carbon. Anal. Bioanal. Chem. 401 (10), 3141–3152.
Feng, Y., Chen, Y., Guo, H., Zhi, G., Xiong, S., Li, J., Sheng, G., Fu, J., 2009. Characteristics of organic and elemental carbon in $PM_{2.5}$ samples in Shanghai, China. Atmos. Res. 92 (4), 434–442.
Fu, X., Wang, S.X., Cheng, Z., Xing, J., Zhao, B., Wang, J.D., Hao, J.M., 2014. Source, transport and impacts of a heavy dust event in the Yangtze River Delta, China, in 2011. Atmos. Chem. Phys. 14 (3), 1239–1254.
Fu, X., Wang, S., Zhao, B., Xing, J., Cheng, Z., Liu, H., Hao, J., 2013. Emission inventory of primary pollutants and chemical speciation in 2010 for the Yangtze River Delta region, China. Atmos. Environ. 70, 39–50.
Gao, L., Jia, G., Zhang, R., Che, H., Fu, C., Wang, T., Zhang, M., Jiang, H., Van, P., 2011. Visual range trends in the Yangtze River Delta region of China, 1981–2005. J. Air & Waste Manag. Assoc. 61 (8), 843–849.
Hand, J.L., 2011. Spatial and Seasonal Patterns and Temporal Variability of Haze and its Constituents in the United States, Cooperative Institute for Research in the Atmosphere (CIRA). Colorado State University.
Harper, M., Pacolay, B., Andrew, M.E., 2005. A comparison of X-ray fluorescence and wet chemical analysis for lead on air filters from different personal samplers used in a bronze foundry. J. Environ. Monit. 7 (6), 592–597.
Hua, W., Chen, Z., Jie, C., Kondo, Y., Hofzumahaus, A., Takegawa, N., Chang, C., Lu, K., Miyazaki, Y., Kita, K., 2008. Atmospheric hydrogen peroxide and organic hydroperoxides during PRIDE-PRD'06, China: their concentration, formation mechanism and contribution to secondary aerosols. Atmos. Chem. Phys. 8 (22), 6755–6773.
Huang, X.F., He, L.Y., Xue, L., Sun, T.L., Zeng, L.W., Gong, Z.H., Hu, M., Zhu, T., 2012. Highly time-resolved chemical characterization of atmospheric fine particles during 2010 Shanghai World Expo. Atmos. Chem. Phys. 12 (11), 4897–4907.
Huang, X.-F., Xue, L., Tian, X.-D., Shao, W.-W., Sun, T.-L., Gong, Z.-H., Ju, W.-W., Jiang, B., Hu, M., He, L.-Y., 2013. Highly time-resolved carbonaceous aerosol characterization in Yangtze River Delta of China: composition, mixing state and secondary formation. Atmos. Environ. 64, 200–207.
Kang, H., Zhu, B., Su, J., Wang, H., Zhang, Q., Wang, F., 2013. Analysis of a long-lasting haze episode in Nanjing, China. Atmos. Res. 120, 78–87.
Liu, X., Gao, T., Liu, L., Zhang, W., Yang, S., Li, T., Taichang, G., Lei, L., Wei, Z., Shuchen, Y., Tao, L., 2010. Influences of precipitation on atmospheric extinction coefficient and visibility. J. Appl. Meteorol. Sci. 21 (4), 433–441.
Lowenthal, D.H., Kumar, N., 2003. $PM_{2.5}$ mass and light extinction reconstruction in IMPROVE. J. Air & Waste Manag. Assoc. 53 (9), 1109–1120.
Pan, H., Geng, F., Chen, Y., He, Q., Zhang, H., Kang, Y., Mao, X., Wang, H., 2010. Analysis of a haze event by micro-pulse light laser detection and ranging measurements in Shanghai. Acta Sci. Circumstantiae 30 (11), 2164–2173.
Pathak, R.K., Wu, W.S., Wang, T., 2009. Summertime $PM_{2.5}$ ionic species in four major cities of China: nitrate formation in an ammonia-deficient atmosphere. Atmos. Chem. Phys. 9 (5), 1711–1722.
Pitchford, M., Malm, W., Schichtel, B., Kumar, N., Lowenthal, D., Hand, J., 2007. Revised algorithm for estimating light extinction from IMPROVE particle speciation data. J. Air & Waste Manag. Assoc. 57 (11), 1326–1336.

Qi, H., Lin, W., Xu, X., Yu, X., Ma, Q., 2012. Significant downward trend of SO_2 observed from 2005 to 2010 at a background station in the Yangtze Delta region, China. Sci. China Chem. 55 (7), 1451–1458.
Qing, Z., Jun, S., 2010. Study on the influencing factors of haze weathers in shanghai. J. Arid Meteorol. 30 (3), 367–373.
Tan, J.H., Duan, J.C., Chen, D.H., Wang, X.H., Guo, S.J., Bi, X.H., Sheng, G.Y., He, K.B., Fu, J.M., 2009. Chemical characteristics of haze during summer and winter in Guangzhou. Atmos. Res. 94 (2), 238–245.
Wang, Y., Li, L., Chen, C., Huang, C., Huang, H., Feng, J., Wang, S., Wang, H., Zhang, G., Zhou, M., Cheng, P., Wu, M., Sheng, G., Fu, J., Hu, Y., Russell, A.G., Wumaer, A., 2014a. Source apportionment of fine particulate matter during autumn haze episodes in Shanghai, China. J. Geophys. Res. Atmos. 119 (4), 1903–1914.
Wang, Y., Zhuang, G., Zhang, X., Huang, K., Xu, C., Tang, A., Chen, J., An, Z., 2006. The ion chemistry, seasonal cycle, and sources of $PM_{2.5}$ and TSP aerosol in Shanghai. Atmos. Environ. 40 (16), 2935–2952.
Wang, X., Chen, W., Chen, D., Wu, Z., Fan, Q., 2014b. Long-term trends of fine particulate matter and chemical composition in the Pearl River Delta Economic Zone (PRDEZ), China. Front. Environ. Sci. Eng. 1–10.
Wei, L., Duan, J., Tan, J., Ma, Y., He, K., Wang, S., Huang, X., Zhang, Y., 2015. Gas-to-particle conversion of atmospheric ammonia and sampling artifacts of ammonium in spring of Beijing. Sci. China Earth Sci. 58 (3), 345–355.
Wu, L., Shen, J., Feng, Y., Bi, X., Jiao, L., Liu, S., 2014. Source apportionment of particulate matters in different size bins during hazy and non-hazy episodes in hangzhou city. Res. Environ. Sci. 27 (4), 373–381.
Xiao, Z., Zhang, Y., Hong, S., Bi, X., Jiao, L., Feng, Y., Wang, Y., 2011. Estimation of the main factors influencing haze, based on a long-term monitoring campaign in Hangzhou, China. Aerosol Air Qual. Res. 11 (7), 873–882.
Yang, F., He, K., Ye, B., Chen, X., Cha, L., Cadle, S.H., Chan, T., Mulawa, P.A., 2005. One-year record of organic and elemental carbon in fine particles in downtown Beijing and Shanghai. Atmos. Chem. Phys. 5 (6), 1449–1457.
Yang, F., Tan, J., Zhao, Q., Du, Z., He, K., Ma, Y., Duan, F., Chen, G., 2011. Characteristics of $PM_{2.5}$ speciation in representative megacities and across China. Atmos. Chem. Phys. 11 (11), 5207–5219.
Yao, X., Chan, C.K., Fang, M., Cadle, S., Chan, T., Mulawa, P., He, K., Ye, B., 2002. The water-soluble ionic composition of $PM_{2.5}$ in Shanghai and Beijing,. China. Atmos. Environ. 36 (26), 4223–4234.
Ye, B., Ji, X., Yang, H., Yao, X., Chan, C.K., Cadle, S.H., Chan, T., Mulawa, P.A., 2003. Concentration and chemical composition of $PM_{2.5}$ in Shanghai for a 1-year period. Atmos. Environ. 37 (4), 499–510.
Zhang, X.Y., Wang, Y.Q., Niu, T., Zhang, X.C., Gong, S.L., Zhang, Y.M., Sun, J.Y., 2012. Atmospheric aerosol compositions in China: spatial/temporal variability, chemical signature, regional haze distribution and comparisons with global aerosols (vol 12, pg 779, 2012). Atmos. Chem. Phys. 12 (14), 6273–6273.
Zhao, X., Zhao, P., Xu, J., Meng, W., Pu, W., Dong, F., He, D., Shi, Q., 2013. Analysis of a winter regional haze event and its formation mechanism in the North China Plain. Atmos. Chem. Phys. 13 (11), 5685–5696.